

New Pyridine-Based Imines to Treat Diabetes Mellitus Targeting α -Glucosidase: In Silico Design, Docking And In Vitro Biological Evaluation

Amit Patel¹, Neha D. Kawathekar² Gaurav Jain³

¹PG student, ²Professor, ³Assistant Professor

^{1,2,3}Department of Pharmacy, Shree Govindram Sakseria Institute of Science and Technology, Indore, Madhya Pradesh, India

ABSTRACT: A novel series of pyridine-based imines were rationally designed and synthesized as anti-diabetic agents. Out of all the synthesized compounds, 3 compounds were selected and were screened for possible α -glucosidase inhibitory potential at two concentrations (1 μ M and 10 μ M) wherein they exhibited α -glucosidase inhibition in the range of 21.23%-36.67% at 1 μ M concentration and 38.42%-52.31% at 10 μ M in comparison with acarbose as the positive control which showed an inhibition of 53.34% at 1 μ M concentration and of 72.56% at 10 μ M concentration. VR3 was the most potent derivative, bearing 4-Chloro moiety. Additionally, the molecular docking of all derivatives was performed to get an insight into the binding mode of these derivatives within the active site of the enzyme. In silico assessments exhibited that all the designed compounds were well occupied in the binding pocket of the enzyme through favorable interactions with various amino acid residues in the active site, correlating to the experimental results.

KEYWORDS: α -glucosidase inhibition, Acarbose, Pyridine, Imines, Molecular docking

INTRODUCTION

One of the most prevalent metabolic degenerative illnesses in the world is diabetes mellitus (DM), which is defined by excessive blood glucose levels.[1]

Retinopathy, neuropathy, amputation, and Charcot's joints are some of the long-term effects of diabetes mellitus. Patients with diabetes are more likely to develop peripheral, cardiovascular, as well as cerebral vascular diseases[2]

According to the International Diabetes Federation, the number of cases of diabetes worldwide increased to 537 million in 2021 from 108 million in 1980 and is projected to reach 642 million by 2040. Prevalence has risen more quickly in developing and underdeveloped nations compared to developed countries.[3] DM requires long-term management because it is a chronic condition, so research into new, efficient, and safer treatments must be done over time. The use of biguanides, thiazolidinediones, and sulfonylureas are a few of the known management techniques.[4]

Reducing meal-derived glucose absorption is another efficient method for reducing postprandial hyperglycemia.[5]

ALPHA-Glucosidase (ALPHA-D-glucoside glucohydrolase, EC 3.2.1.20) resides on the brush borders of the small intestine is an exocarbohydase that catalyzes the breakdown of alpha-glucose from carbohydrates and is involved in maltose catabolism.[6] Because these enzymes are involved in sugar metabolism, ALPHA-glucosidase suppression plays a part in the management of obesity as well as diabetes by preventing carbohydrates from being digested in diabetes.[7] Oral antidiabetic medications that inhibit ALPHA-glucosidase are used to treat diabetes. Moreover, the therapy for diabetes, cancer, HIV/AIDS, and other degenerative diseases depends heavily on the inhibition of alpha-glucosidases and associated enzymes.[8]

According to a number of X-ray crystallographic investigations on complexes with substrates and inhibitors, glucosidases can be inhibited by the enzymatic hydrolysis of glucosidases. This inhibition occurs in a two-step process where a covalent glycosyl-enzyme intermediate is created and hydrolyzed using transition states that resemble oxocarbenium ions.[9]

A thorough study over the past 20 years has led to the discovery of numerous alpha-glucosidase inhibitors, both of synthetic and natural origin. Only a small number, nevertheless, have entered clinical usage and are known to have various negative side effects and decreased efficacy.[10] Among the most important known candidates that are frequently used to inhibit the alpha-glucosidases are acarbose 1-deoxyirimycin (NOJ), miglitol, and voglibose (Fig.1). These inhibitors have side effects and absorptivity issues and therefore, research into novel α -glucosidase inhibitors is both important and intriguing.[11]

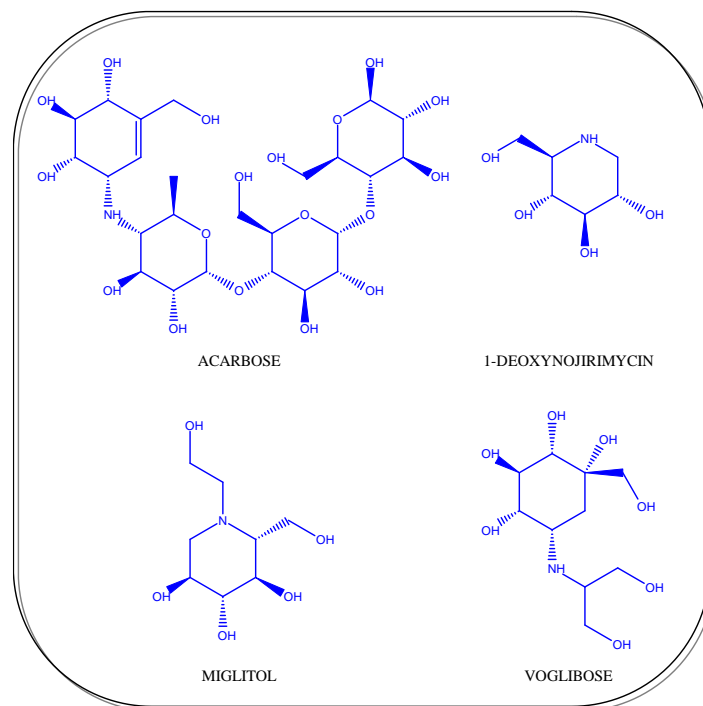


Fig.1 – Inhibitors of alpha-glucosidase

Pyridine, with the chemical formula C_5H_5N is a basic heterocyclic organic compound which is a benzene bio isostere with one methine group ($=CH$) replaced by a nitrogen atom.[12]

Pyridine scaffolds are known for their antimicrobial, antiviral, antioxidant, anti-inflammatory, antiamoebic, antidiabetic, antimalarial, and anti-psychotic medicinal properties; as a result, they are used in many drugs and have been found to improve the pharmacological properties of the drugs due to their low basicity and aqueous solubility.[13] Therefore, Pyridine nucleus was selected for further modification to synthesize alpha-glucosidase inhibitors.

According to literature the most widely accepted theory for how alpha-glucosidase enzyme-catalyzed processes are inhibited involves a proton transfer mechanism of some kind.[14] Because of the basic lone pair of electrons on the nitrogen atom, pyridines are also well-known catalysts.[15] They can exist in both protonated and deprotonated forms, and their catalytic potential has been investigated in a number of chemical transformations. The pyridine scaffold may be able to inhibit -glucosidase through a reversible protonation and deprotonation mechanism.[16]

An imine is a functional group or organic compound that contains a carbon-nitrogen double bond ($C=N$). The nitrogen atom can be linked to either a hydrogen or an organic group (R). There are two more single bonds on the carbon atom.[17] Imines have become more and more popular in the medical and pharmaceutical industries due to a variety of biological activities including anti-inflammatory, analgesic, antimicrobial, anticonvulsant, antitubercular, anticancer, antioxidant, anthelmintic, and others.[18]

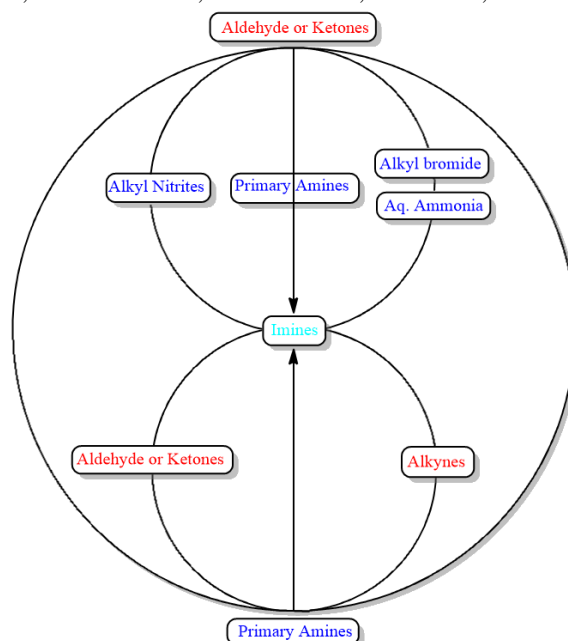


Fig.2- Synthetic Approaches for Imines.

In recent years, significant progress has been made in the synthesis of imines, which have been prepared using various methods from aldehydes and/or amines and their chemical equivalents. As shown in Fig.2, these methods include condensation of aldehydes/ketones with amines addition of aryl halides and liquid ammonia to aldehydes/ketones, hydroamination of alkynes, oxidative coupling of amines to give imines, oxidative coupling of alcohols and amines, and dehydrogenation of secondary amines.[19]

In this aspect of medicinal and pharmacological properties of both pyridine scaffold and imine functional group, a novel series of pyridine based imines was synthesized in order to assess its alpha-glucosidase inhibitory potential.

RESULTS AND DISCUSSION

DESIGNING

There are numerous reports in the literature that show pyridine as the scaffold of compounds with potent alpha-glucosidase inhibitory activity, and the imine bond has been shown to have anti-inflammatory, analgesic, antimicrobial, anticonvulsant, antitubercular, anticancer, antioxidant, anthelmintic, and other activities.

With this knowledge, a series of pyridine-based imine hybrids as novel alpha-glucosidase inhibitors were designed and synthesized. In vitro, all derivatives were tested for alpha-glucosidase inhibitory activity. Furthermore, molecular docking studies on all derivatives were carried out to gain insight into the binding affinity and position of these compounds within the enzyme binding site.

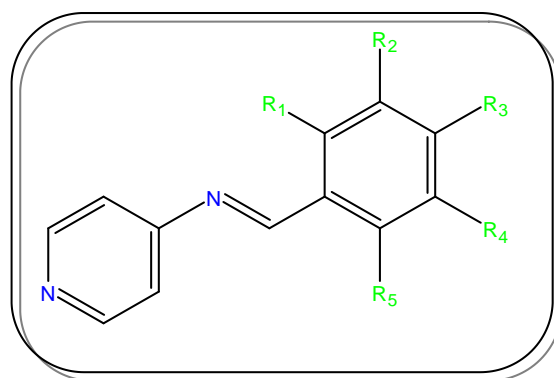
CHEMISTRY

Scheme 1 represents the pathway for the synthesis of the newly designed pyridine-based imine derivatives. These compounds were synthesized through a simple reaction between commercially available 4-amino pyridine and substituted benzaldehydes at equimolar quantities in dry ethanol as a solvent at 70 °C. Since the reaction is reversible in nature and the product can get hydrolyzed to give back the starting materials, it was carried out in a 250 mL three-necked flask fitted with a guard tube containing fused calcium chloride on one neck in order to absorb the evaporating water so as to allow the reaction to run in the forward direction. Also, for highest yield of imine synthesis the reaction pH must be optimized to pH 5, and for that 2-5 drops of acetic acid were added into it to the reaction mixture. Optimized TLC mobile phase in a ratio chloroform: methanol (6:4) was used to monitor the reaction progress. Finally all the synthesized compounds were fully characterized by ¹H NMR, and FT-IR.

BIOLOGICAL ACTIVITIES

The inhibitory potency of all the synthesized pyridine based imines against α -glucosidase at different concentrations (1 μ M and 10 μ M) was evaluated and compared with acarbose as a reference standard and the inhibition by 3 most active inhibitors represented in table 1 along with a graph showing the inhibition by these compounds in 3D representation (Fig.3). All the compounds displayed inhibitory activity against α -glucosidase (α G) except compound VR10, but showed less inhibition potential as compared to the standard, the compounds VR3 was the most active inhibitor of them all having an electron-withdrawing group (EWG) as a substituent. It is observed that a better activity is achieved if R is an electron-withdrawing group (EWG) whereas for the compounds having electron-donating group (EDG) the activity was diminished. Also, the position of the substitution is quite important in determining the activity of the compounds and it is observed that para substituted compounds shows better inhibition as compared to ortho and meta substituted compounds. From these results, it is concluded that pyridine based imines with an EWG could be more active against α GI than those with a EDG as substituent. But they are not as active as the standard drug acarbose and need further research and development.

Table 1. In vitro α -glucosidase inhibitory activities of compounds.



Compound	R ₁	R ₂	R ₃	R ₄	R ₅	Inhibition (in %) At 1 μ M	Inhibition (in %) At 10 μ M
VR3	H	H	Cl	H	H	35.28	52.31
VR4	H	H	N(CH ₃) ₂	H	H	32.18	44.28
VR9	H	H	OH	H	H	36.67	48.62

Acarbose	-	-	-	-	-	53.34	72.56
----------	---	---	---	---	---	-------	-------

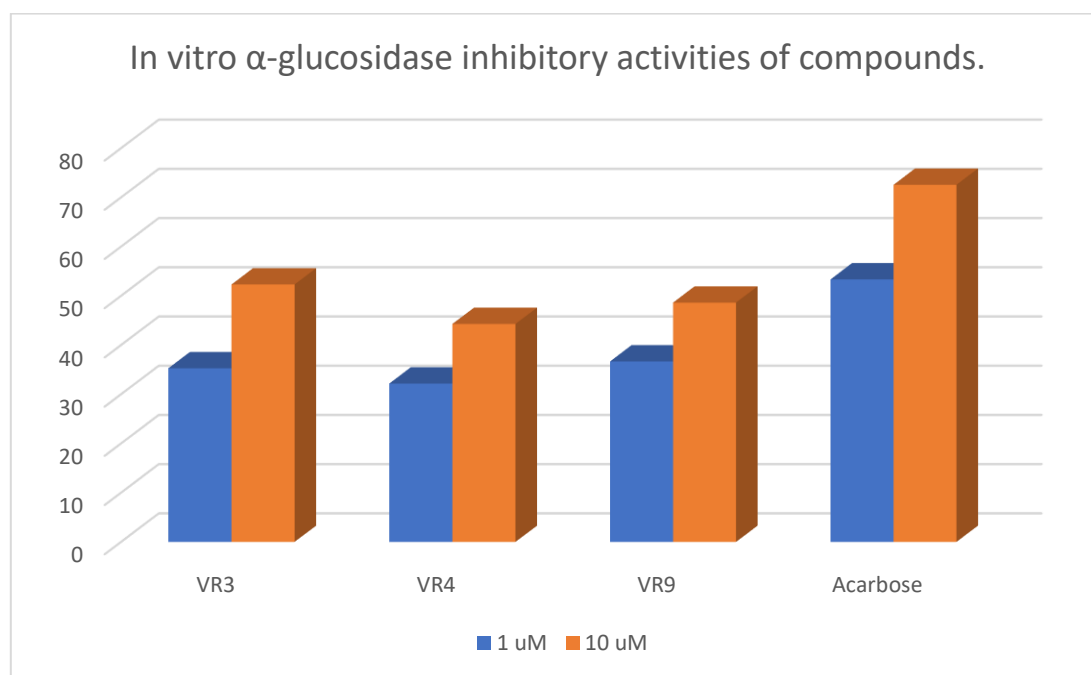


Fig.3 -3D-cluster column representation of table 1

MOLECULAR DOCKING

Next, the molecular docking studies of all derivatives were performed. In the first step, to properly predict the binding pose of derivatives within the active site, the redocking process of NOJ (as a crystallographic ligand) with human lysosomal acid- α -glucosidase was performed using Autodock vina. Alignment of the best pose of NOJ in the active site of α -glucosidase and crystallographic ligand recorded an RMSD value of 0.4 Å. Fig 4 represents the superimposed crystallographic NOJ and docked NOJ structures in the active site of the protein. On validation of the docking protocol the same was used for the reference drug acarbose as well as all the other ligand docking.

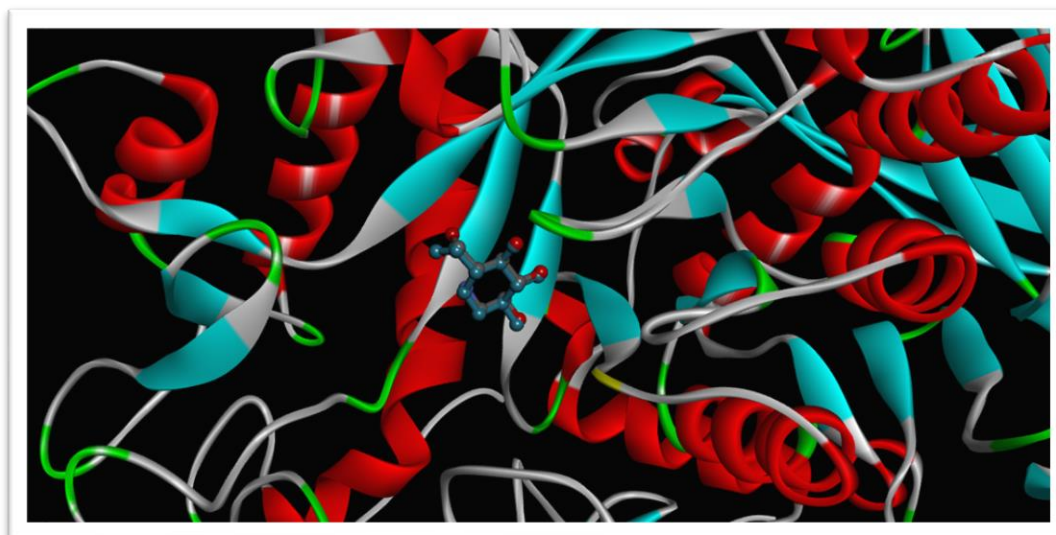


Fig 4 -Superimposed Crystallographic NOJ and docked NOJ structures in the active site of the protein(5nn5)

The binding energy values between ligand and target proteins after docking have been mentioned in Table 3. The results revealed that all ligands were well accommodated in the protein pockets of alpha-glucosidase. The molecular docking analysis of the standard drug acarbose with the protein pocket of alpha-glucosidase is demonstrated in Figure 5. The stable conformation of acarbose and alpha-glucosidase complex showed the lowest binding energy of -6.8 kcal/mol. Acarbose was stabilized in the protein pocket of alpha-glucosidase involving many conventional hydrogen bonding and van der Waals forces. 6 different hydrogen bonds were observed between hydroxyl functional groups of acarbose and amino acids ASP:404, ASP:518, ASP:616 ARG:195, TRY:481, GLY A:651, and SER A:679, respectively.



Fig.5-3D interaction pattern of acarbose within the α -glucosidase active site

Also, the co-crystal structure NOJ was stabilized in the protein pocket of alpha-glucosidase involving conventional hydrogen bonding using hydroxyl functional groups and amino acids ASP:518, ASP:616, MET:519, ARG:600. The lowest binding energy of the VR3-alpha-glucosidase complex was -4.7 kcal/mol.

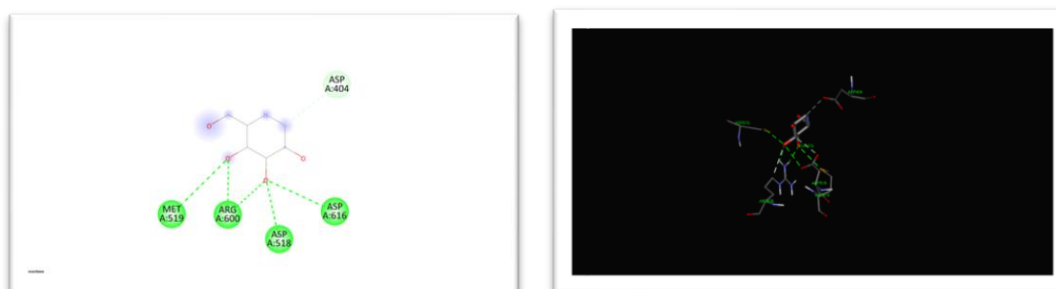


Fig.6-3D interaction pattern of NOJ within the α -glucosidase active site

VR3

The lowest binding energy of the VR3-alpha-glucosidase complex was -6.5 kcal/mol. It is one of the 3 best inhibitors synthesized. The nitrogen of the pyridine ring showed conventional hydrogen bonding with HIS A:674. whereas the pyridine ring further stabilized the protein-ligand complex by establishing carbon-hydrogen bonding and Pi-anion bonding with amino acids ASP A:404 and ASP A:518. The aromatic ring of the ligand was stabilized by hydrophobic contact through Pi-Pi stacking with amino acid TRP A:481. The methyl groups also developed Pi-alkyl interactions with amino acid PHE A:525. Furthermore, the carbon in the imine bond developed carbon-hydrogen bonding with ASP A:616.

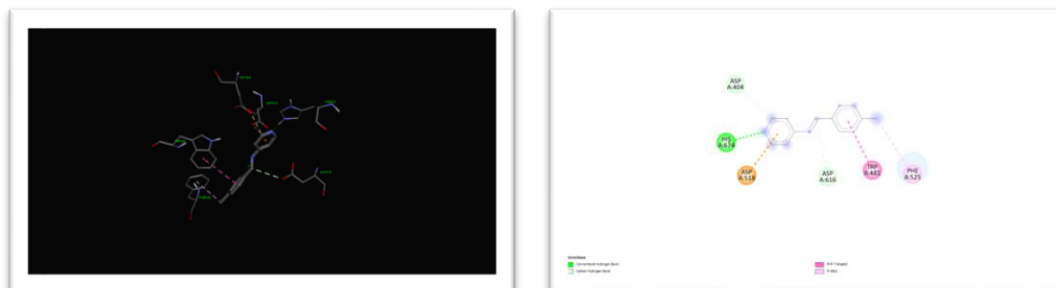


Fig.7-3D interaction pattern of compounds VR3 within the α -glucosidase active site

VR4

The lowest binding energy of the VR3-alpha-glucosidase complex was -6.5 kcal/mol. The nitrogen of the imine bond showed conventional hydrogen bonding with ARG A:600. whereas the pyridine ring further stabilized the protein-ligand complex by establishing Pi-carbon bonding with amino acids ASP A:518 and ASP A:616. The aromatic ring of the ligand was stabilized by hydrophobic contact through Pi-carbon bonding with amino acids ASP A:282 along with Pi-anion bonding with amino acids ARG A:600.

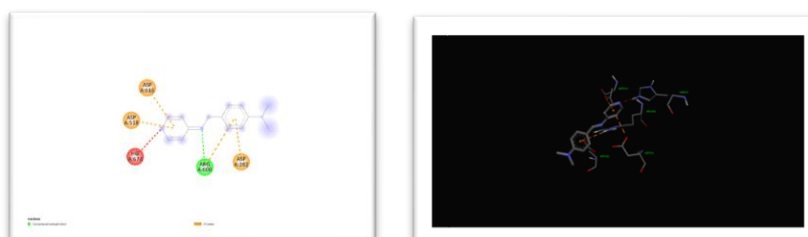


Fig.8-3D interaction pattern of compounds VR4 within the α -glucosidase active site

VR9

The lowest binding energy of the VR3- α -glucosidase complex was -6.6 kcal/mol.

Phenolic -OH group of the ligand VR9 established stronger conventional hydrogen bonds with 2 amino acid residues ASP A:404 and HIS A:674. The phenyl ring was stabilized in the complex through hydrophobic Pi-Pi stacking with amino acids TRP A:367 and PHE A:649 along with a Pi-anion bonding with amino acids ASP A:518. Whereas, the pyridine ring established a Pi-anion bonding with amino acids ASP A:282.

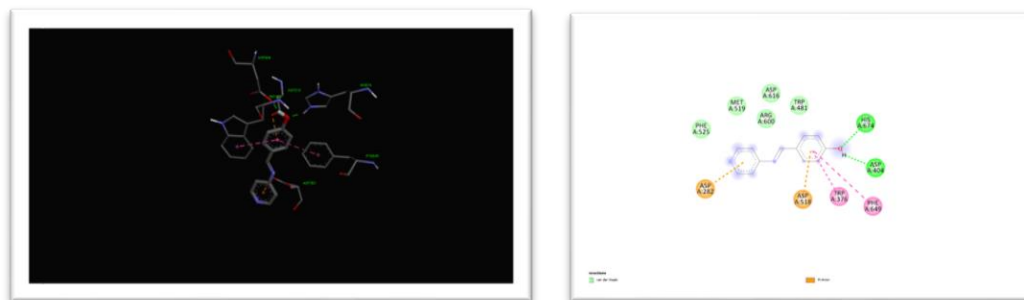


Fig.9-3D interaction pattern of compounds VR9 within the α -glucosidase active site

DISCUSSION

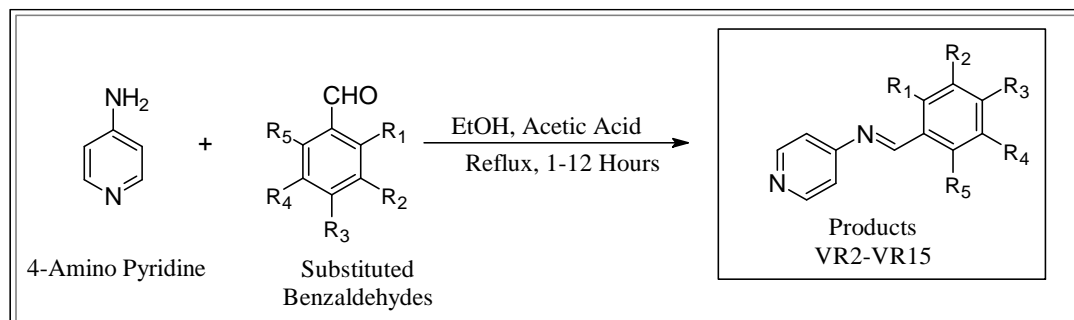
Under microwave solvent-free conditions, an easy, efficient, and environmentally friendly method for the synthesis of aryl imines using ASA as a heterogeneous catalyst was developed. This method provides aryl imines in a short period of time using a simple workup procedure while avoiding purification methods for the final products. The molecular docking results encourage us to create novel aryl imines with potential anti-diabetic properties as well as improved efficiency and selectivity. The aryl imines 3d, 3f, and 3i have potential for in vivo antidiabetic evaluations, according to the results of in vitro tests and molecular docking studies.

EXPERIMENTAL**CHEMISTRY**

10 new Pyridine based imine derivatives were synthesized in our lab following the synthetic schemes shown in fig. to yield the final products. Thin layer Chromatography (TLC) (Merck 60F254 silica gel plates supported on aluminum) was used to monitor the progress of the reaction. The TLC plates were visualized under short-wave (254nm) or long-wave (365nm) ultraviolet light. The Infrared spectroscopy of all the synthesized was carried out on IR Prestige-21 using the KBr pellet technique in School of Pharmaceutical Science, Rajiv Gandhi Proudyogiki Vishwavidyalaya Bhopal (M.P) and are expressed in cm^{-1} . ^1H NMR of synthesized compound was recorded in 500MHz NMR facility at Department of Chemistry, Indian Institute of Technology, Indore using CDCl_3 as solvent and TMS as internal standard.

General procedure for the synthesis of pyridine based imines

0.01 mol of 4-Amino-pyridine (0.94 grams) was dissolved in 10 mL of ethanol in a 250 mL three-necked flask fitted with a guard tube containing fused calcium chloride on one neck and was stirred at room temperature for 15 min to dissolve the 4-amino pyridine and get a clear solution. To this solution, an equimolar quantity (0.01 mol) of each substituted aryl aldehyde (in Ethanol) was added and 2-5 drops of acetic acid was added into it to adjust the pH to 5. The Reaction mixture was then refluxed with stirring at 70°C on a magnetic stirrer for for time period shown in Table no. . The reaction progress was monitored by TLC using mobile phase as chloroform: methanol (6:4). On completion of the reaction the product was allowed to cool to normal temperature and then kept in an ice bath until solid precipitates. The solid precipitate was washed using diethyl ether and was then recrystallized using ethanol to give pure products.



Scheme 1.- General procedure for the synthesis of pyridine-based imines

VR2 [(E)-N-benzylidenepyridine-4-amine]

According to general procedure, VR2 was obtained from 4-Amino pyridine, benzaldehyde, in 8 hr with 56% yield as light orange crystalline solid: m.p. $170-172^\circ\text{C}$; RF 0.28 (Chloroform: Methanol: TEA (6: 3.9: 0.1)); ^1H NMR (500 MHz, CDCl_3) δ 1.16 (s, 1H),

0.80 – 0.74 (m, 1H), 0.62 – 0.54 (m, 3H), 0.22 – 0.10 (m, 6H), 0.01 – -0.12 (m, 4H). $\nu_{\max}/\text{cm}^{-1}$ (KBr): 1815.09 (C-H (Bending - Aromatic)), 3029.34 (C-H (Stretching - Alkene)), 1647.28 (C=C), 1694.54 (C=N (imine)).

VR3 [(E)-N-(4-Chlorobenzylidene) pyridine-4-amine]

According to general procedure, VR2 was obtained from 4-Amino pyridine, 4-Chlorobenzaldehyde, in 7 hr with 63.90 % yield as orange crystalline solid: m.p. 103-105 °C; RF 0.56 (Chloroform: Methanol (5: 5)); ¹H NMR (500 MHz, CDCl₃) δ 8.46 (s, 1H), 7.95 – 7.87 (m, 2H), 7.53 – 7.44 (m, 3H), 7.43 – 7.31 (m, 2H), 7.27 – 7.19 (m, 3H). $\nu_{\max}/\text{cm}^{-1}$ (KBr): 1816.06 (C-H (Bending - Aromatic)), 3126.74 (C-H (Stretching - Alkene)), 659.68 (C-Cl (Halide)), 1612.56 (C=C), 1692.61 (C=N (imine))

VR4 [(E)-N-(4-(dimethyl amino) benzylidene) pyridine-4-amine]

According to general procedure, VR2 was obtained from 4-Amino pyridine, Para-dimethylaminobenzaldehyde, in 3 hr with 75.50 % yield as white crystalline solid: m.p. 225-230 °C; RF 0.52 (Chloroform: Methanol: TEA (6: 3.9: 0.1)); ¹H NMR (500 MHz, CDCl₃) δ 8.32 (s, 1H), 7.80 – 7.71 (m, 2H), 7.40 – 7.33 (m, 1H), 7.22 – 7.14 (m, 2H), 6.75 (s, 1H), 6.71 (d, J = 16.0 Hz, 1H), 3.09 (s, 1H), 3.05 (s, 4H), 1.65 – 1.61 (m, 1H). $\nu_{\max}/\text{cm}^{-1}$ (KBr): 1820.86 (C-H (Bending - Aromatic)), 2867.31 (C-H (Stretching - Alkane)), 3097.81 (C-H (Stretching - Alkene)), 1663.68 (C=C), 1682 (C=N (imine)), 3501.92 (C-N (amine))

VR7 [(E)-N-(2-Chlorobenzylidene) pyridine-4-amine]

According to general procedure, VR2 was obtained from 4-Amino pyridine, 2-Chloro benzaldehyde, in 7 hr with 42.20 % yield as off white crystalline solid: m.p. 205-210 °C; RF 0.51 (Chloroform: Methanol (5: 5)); ¹H NMR (500 MHz, CDCl₃) δ 8.25 (dd, J = 20.1, 5.7 Hz, 3H), 7.41 – 7.29 (m, 1H), 6.54 (dt, J = 6.0, 2.8 Hz, 2H), 6.50 – 6.46 (m, 1H), 4.81 (s, 1H), 4.23 (s, 2H), 2.10 – 2.06 (m, 1H), 1.96 (s, 5H). $\nu_{\max}/\text{cm}^{-1}$ (KBr): 1827.63 (C-H (Bending - Aromatic)), 3499 (OH- Aromatic), 1601.95 (C=C), 1694.54 (C=N (imine))

VR9 [(E)-4-((pyridine-4-ylimino) methyl) phenol]

According to general procedure, VR2 was obtained from 4-Amino pyridine, 4-Hydroxybenzaldehyde, in 6 hr with 66.50 % yield as light brown crystalline solid: m.p. 98-100 °C; RF 0.25 (Chloroform: Methanol (5: 5)); ¹H NMR (500 MHz, CDCl₃) δ 8.38 (s, 1H), 7.84 – 7.78 (m, 2H), 7.42 – 7.35 (m, 2H), 7.25 – 7.16 (m, 3H), 6.95 – 6.88 (m, 2H), 5.37 (s, 1H). $\nu_{\max}/\text{cm}^{-1}$ (KBr): 1807 (C-H (Bending - Aromatic)), 659.68 (C-Cl (Halide)), 1612.56 (C=C), 1692.61 (C=N (imine))

VR10 [(Z)-N-(2-phenylethylidene) pyridine-4-amine]

According to general procedure, VR2 was obtained from 4-Amino pyridine, Cinnamaldehyde, in 1 hr with 72.60 % yield as orange crystalline solid: m.p. 160-165 °C; RF 0.54 (Chloroform: Methanol: TEA (6: 3.9: 0.1)); ¹H NMR (500 MHz, CDCl₃) δ 8.28 (d, J = 7.8 Hz, 1H), 7.58 – 7.51 (m, 2H), 7.44 – 7.30 (m, 5H), 7.26 – 7.07 (m, 5H). $\nu_{\max}/\text{cm}^{-1}$ (KBr): 1834.06 (C-H (Bending - Aromatic)), 2863.45 (C-H (Stretching - Alkane)), 3121.92 (C-H (Stretching - Alkene)), 1612.56 (C=C), 1697.43 (C=N (imine))

VR12 [(E)-N-(3-Chlorobenzylidene) pyridine-4-amine]

According to general procedure, VR2 was obtained from 4-Amino pyridine, 3-Chlorobenzaldehyde, in 7 hr with 63.50 % yield as off white crystalline solid: m.p. 165-170 °C; RF 0.68 (Chloroform: Methanol (5: 5)); ¹H NMR (500 MHz, CDCl₃) δ 9.99 (s, 1H), 8.25 (dd, J = 21.9, 6.0 Hz, 2H), 7.83 (d, J = 8.4 Hz, 1H), 7.52 (d, J = 8.4 Hz, 1H), 7.43 (t, J = 8.4 Hz, 1H), 7.27 (d, J = 3.0 Hz, 2H), 6.55 – 6.51 (m, 1H), 6.46 (d, J = 6.1 Hz, 1H), 4.12 (s, 1H). $\nu_{\max}/\text{cm}^{-1}$ (KBr): 1822.81 (C-H (Bending - Aromatic)), 3037.05 (C-H (Stretching - Alkene)), 659.68 (C-Cl (Halide)), 1615.45 (C=C), 1691.64 (C=N (imine))

VR13 [(E)-3-((pyridine-4-ylimino) methyl) phenol]

According to general procedure, VR2 was obtained from 4-Amino pyridine, 3-Hydroxybenzaldehyde, in 6 hr with 50.40 % yield light yellow crystalline solid: m.p. 120-125 °C; RF 0.61 (Chloroform: Methanol (5: 5)); ¹H NMR (500 MHz, CDCl₃) δ 8.38 (s, 1H), 7.81 (dd, J = 8.8, 2.3 Hz, 3H), 7.42 – 7.35 (m, 2H), 7.29 – 7.16 (m, 4H), 6.98 – 6.89 (m, 3H). $\nu_{\max}/\text{cm}^{-1}$ (KBr): 1806.41 (C-H (Bending - Aromatic)), 3033.19 (C-H (Stretching - Alkene)), 3502.88 (OH - Aromatic), 1694.54 (C=N (imine))

VR14 [(E)-N-(4-methylamino) benzylidene) pyridine-4-amine]

According to general procedure, VR2 was obtained from 4-Amino pyridine, 4-Methylbenzaldehyde, in 12 hr with 52.50 % yield off crystalline solid: m.p. 150-155 °C; RF 0.41 (Chloroform: Methanol: TEA (6: 3.9: 0.1)); ¹H NMR (500 MHz, CDCl₃) δ 8.22 (dd, J = 4.9, 3.0 Hz, 2H), 6.52 (dq, J = 4.6, 1.5 Hz, 2H), 4.11 (s, 2H), 1.78 (s, 1H). $\nu_{\max}/\text{cm}^{-1}$ (KBr): 1819.92 (C-H (Bending - Aromatic)), 1628.95 (C-H (Stretching - Alkane)), 3039.95 (C-H (Stretching - Alkene)), 1628.55 (C=C), 1697.43 (C=N (imine))

VR15 [(E)-N-(3-methylbenzylidene) pyridin-4-amine]

According to general procedure, VR2 was obtained from 4-Amino pyridine, 4-Methylbenzaldehyde, in 7.5 hr with 55.50 % yield as orange crystalline solid: m.p. 175-180 °C; RF 0.24 (Chloroform: Methanol: TEA (6: 3.9: 0.1)); ¹H NMR (500 MHz, CDCl₃) δ 9.74 (d, J = 1.9 Hz, 2H), 8.24 – 8.19 (m, 1H), 7.78 – 7.71 (m, 4H), 6.74 – 6.68 (m, 4H), 6.55 – 6.50 (m, 1H), 4.16 (s, 1H), 3.09 (d, J = 1.7 Hz, 12H), 1.98 (s, 1H). $\nu_{\max}/\text{cm}^{-1}$ (KBr): VR15 [(E)-N-(3-methylbenzylidene) pyridin-4-amine], IR- 1823.01 (C-H (Bending - Aromatic)), 3277.20 (C-H (Stretching - Alkane)), 3034.16 (C-H (Stretching - Alkene)), 1691.94 (C=N (imine))

In vitro alpha-glucosidase inhibitory activity

The alpha-glucosidase (EC 3.2.1.20) activity of synthetic quinazoline-2,4(1H,3H)-diones was determined using the method described by Kwon et al., [20] with minor modifications. 100 L of the enzyme solution (1 U mL⁻¹ in 0.1 M of phosphate buffer at pH 7.0) and 50 L of pyridine based imine solution (concentrations of 1 μ M, and 10 μ M in methanol) were added to a 96-well flat-

bottom plate. After 10 minutes at 25 °C, 50 L of 5 mM p-nitro-phenyl—D-glucopyranoside solution in 0.1 M phosphate buffer (pH 7.0) was added and incubated for 5 minutes at 25 °C. The absorbance was then measured at 405 nm with a microplate reader. The inhibitory activity of alpha -glucosidase was expressed as a percentage of inhibition and was calculated as follows::

$$\% \text{ Inhibition} = \frac{\text{Abscontrol} - \text{Absamples}}{\text{Abscontrol}} \times 100$$

Where Abscontrol was the absorbance without sample, Absamples was the absorbance of the sample at different concentrations.

Molecular docking studies

The AutoDock Tool v1.5.7 was used to direct the automated molecular docking studies to the active site of the enzyme. To begin, ChemDraw Ultra V12 was used to create the pyridine-based imines (ligands), followed by Chem 3D Pro V12 for 3D optimization with MM2 to achieve the lowest energy geometry, including the water phase. The ligands were assigned Gasteiger charges after the structures were saved as SYBYL mol2 files. Second, human lysosomal acid—glucosidase crystal structures was obtained from the RCSB protein data bank (pdb code: 5NN5). All water molecules, ligands, and cations were removed from the protein prior to docking calculations. Polar hydrogens and Kollman charges were later assigned to the protein.

Discovery Studio Visualizer v17.2.0.16349 and Pymol were used to examined the conformation with the lowest binding energy to determine binding orientations, molecular modelling, hydrogen bond evaluation, and other interactions.

REFERENCE

- Zhen, J., et al., *Synthesis of novel flavonoid alkaloids as α -glucosidase inhibitors*. Bioorg Med Chem, 2017. **25**(20): p. 5355-5364.
- Diagnosis and classification of diabetes mellitus*. Diabetes Care, 2009. **32 Suppl 1**(Suppl 1): p. S62-7.
- Bhurosy, T. and R. Jeewon, *Overweight and obesity epidemic in developing countries: a problem with diet, physical activity, or socioeconomic status?* ScientificWorldJournal, 2014. **2014**: p. 964236.
- Saeedi, P., et al., *Global and regional diabetes prevalence estimates for 2019 and projections for 2030 and 2045: Results from the International Diabetes Federation Diabetes Atlas, 9(th) edition*. Diabetes Res Clin Pract, 2019. **157**: p. 107843.
- Hiyoshi, T., M. Fujiwara, and Z. Yao, *Postprandial hyperglycemia and postprandial hypertriglyceridemia in type 2 diabetes*. J Biomed Res, 2017. **33**(1): p. 1-16.
- Lin, A., B.-H. Lee, and W.-J. Chang, *Small intestine mucosal α -glucosidase: A missing feature of in vitro starch digestibility*. Food Hydrocolloids, 2015. **53**.
- Hossain, U., et al., *An overview on the role of bioactive α -glucosidase inhibitors in ameliorating diabetic complications*. Food Chem Toxicol, 2020. **145**: p. 111738.
- Avci, D., et al., *Novel Cu(II), Co(II) and Zn(II) metal complexes with mixed-ligand: Synthesis, crystal structure, α -glucosidase inhibition, DFT calculations, and molecular docking*. 2019. **1197**: p. 645-655.
- Davies, G.J., et al., *Snapshots along an Enzymatic Reaction Coordinate: Analysis of a Retaining β -Glycoside Hydrolase*. Biochemistry, 1998. **37**(34): p. 11707-11713.
- Groopman, J.E., *Current advances in the diagnosis and treatment of AIDS: an introduction*. Rev Infect Dis, 1990. **12**(5): p. 908-11.
- Liu, S.-K., et al., *Discovery of New α -Glucosidase Inhibitors: Structure-Based Virtual Screening and Biological Evaluation*. 2021. **9**.
- Mohamed, E.A., et al., *Medicinal attributes of pyridine scaffold as anticancer targeting agents*. Future Journal of Pharmaceutical Sciences, 2021. **7**(1): p. 24.
- Tahir, T., et al., *Pyridine Scaffolds, Phenols and Derivatives of Azo Moiety: Current Therapeutic Perspectives*. Molecules, 2021. **26**(16).
- Dirir, A.M., et al., *A review of alpha-glucosidase inhibitors from plants as potential candidates for the treatment of type-2 diabetes*. Phytochem Rev, 2022. **21**(4): p. 1049-1079.
- Satyanarayan, P., *Pyridine: A Useful Ligand in Transition Metal Complexes*, in *Pyridine*, P. Pratima Parashar, Editor. 2018, IntechOpen: Rijeka. p. Ch. 5.
- Rehman, T., I. Khan, and S. Riaz, *Novel substituted 3-phenyl 1-(4-(5-bromopyridin-3-yl)-6-phenylpyrimidin-2-yl)-thiourea compounds as key small organic molecules for the potential treatment of type II diabetes mellitus: in vitro studies against yeast α -glucosidase*. Medicinal Chemistry Research, 2017. **26**.
- Choudhury, L.H. and T. Parvin, *Recent advances in the chemistry of imine-based multicomponent reactions (MCRs)*. Tetrahedron, 2011. **67**(43): p. 8213-8228.
- Kajal, A., et al., *Schiff Bases: A Versatile Pharmacophore*. Journal of Catalysts, 2013. **2013**: p. 893512.
- Patil, R.D. and S. Adimurthy, *Catalytic Methods for Imine Synthesis*. Asian Journal of Organic Chemistry, 2013. **2**(9): p. 726-744.
- Kwon, Y.I., E. Apostolidis, and K. Shetty, *In vitro studies of eggplant (Solanum melongena) phenolics as inhibitors of key enzymes relevant for type 2 diabetes and hypertension*. Bioresour Technol, 2008. **99**(8): p. 2981-8.